25th ABCM International Congress of Mechanical Engineering
October 20-25, 2019, Uberlândia, MG, Brazil

COB-2019-1614
ON THE USE OF BLADE-SECTION DATA IN THE PROPELLER LIFTING-LINE THEORY

José Rodolfo Chreim
Marcos de Mattos Pimenta
University of São Paulo - Dept. of Mechanical Engineering. 2231, Prof. Mello Moraes Av. - Cidade Universitária - São Paulo - SP - Brazil
jrchreim@usp.br, mpimenta@usp.br

Fillipe Rocha Esteves
Gustavo de Goes Gomes
Gustavo Roque da Silva Assi
University of São Paulo - Dept. of Naval Architecture and Ocean Engineering. 2231, Prof. Mello Moraes Av. - Cidade Universitária - São Paulo - SP - Brazil
fillipe.esteves@usp.br, gustavo.gomes@usp.br, g.assi@usp.br

João Lucas Dozzi Dantas
Institute for Technological Research. 532, Prof. Almeida Prado - Cidade Universitária - São Paulo - SP - Brazil
jdantas@ipt.br

Abstract. *This paper aims to present a comparison of three sources of bi-dimensional data for the NACA 66 TMB modified a = 0.8 that can be used in a modern lifting-line formulation for the hydrodynamic analysis of propellers, briefly reviewed herein. The sources - experimental/analytic expression, numerical, and theoretical - are compared to one another and later used in the propeller lifting-line to obtain the thrust and torque versus the advance coefficients; the results are compared to both numerical data from full Computational Fluid Dynamics simulations using commercial software Star-CCM+ and experimental data from the Cavitation Tunnel of the Institute for Technological Research, and corroborate the need for adequate choice of the 2-D data for the lifting-line in order to improve the results in comparison to experimental data. Consequently, the proposed formulation, together with appropriate blade sections data, seems comparable to more complex numerical methods that can be used for the same analysis purposes.*

Keywords: *Propeller Lifting-Line, Propeller Analysis, Vortex-Step Method, Hull-Propeller Design, Propeller Hydrodynamics*

1. INTRODUCTION

In the recent years, the knowledge in the emission estimates for greenhouse gases from ships made the International Maritime Organization adopt an Energy Efficiency Design Index for ship design, which inherently requires the choice of efficient propellers for specified hulls. In a purely fluid-dynamic framework, propeller design and analysis is an already intricate process that demands knowledge of propeller hydrodynamics, assisted by several tools that usually differ from one another by a balance between fidelity and cost.

Motivated by such vision and interested in a numerical tool with adequate cost-fidelity balance for preliminary hull-propeller design, Chreim *et al.* (2017, 2018b,a) have been working towards a formulation of the Propeller Lifting-Line (PLL) theory that tries to broaden the use of the original formulation of Lerbs (1952) - limited to propellers with straight half-chord $\left(\frac{c}{2}\right)$ blade lines with moderate Expanded Area Ratio (EAR) subject to potential flows - without recurring to the LS corrections of Morgan *et al.* (1968) to improve the thrust (K_T) and torque (K_Q) coefficient estimates. Since modern propellers take advantage of the improvements offered by the inclusion of rake and skew, and since the influence of viscosity on thrust and torque cannot be neglected, a more general formulation is interesting.

Thus, a novel PLL had been proposed, inspired in the advances in the Wing Lifting-Line (WLL) throughout the years (Pistolesi, 1937; Weissinger, 1947; Pepper and van Dam, 1996; Phillips and Snyder, 2000; Katz and Plotkin, 2001; de Souza, 2005; Chreim *et al.*, 2018b) in an attempt to expand the original Lanchester-Prandtl lifting-line theory to the analysis of swept and dihedral wings under the influence of viscosity on the wing lift and drag. The PLL formulation incorporated such adaptations, as corroborated by verification (Chreim *et al.*, 2018a) and validation procedures (Chreim

et al., 2019); however, the validation only used 2-D experimental/analytic data from a NACA 66 foil family (Brockett, 1966) as the source of blade section lift C_n and drag C_c coefficients. Because not all foil families have appropriate expressions for C_n and C_c as function of the angle of attack α, the use of 2-D Computational Fluid Dynamics (CFD) are options for obtaining $C_n \times \alpha$ and $C_c \times \alpha$ curves. Therefore, the present paper deals with a comparison among the outputs of the PLL for three different sources of 2-D data, and these results are also compared to both full CFD simulations and experimental data for a propeller called MOD5.

2. Overview of the Formulation

An overview of the linear and a nonlinear schemes detailed in Chreim *et al.* (2018a) is presented accompanied by a minor change in the calculation of the hydrodynamic pitch angles (Chreim *et al.*, 2019); each blade and its wake is discretized by N helical horseshoe vortices (HHSV) placed alongside (Figure 1) in a Vortex-Step fashion, with their bound vortices placed along the quarter chord line and the CPs initially placed along the three-quarter chord line; moreover, while part of the HHSVs remains over the blade planform, the other part is shed downstream following an assumed constant pitch helical path.

3. OVERVIEW OF THE FORMULATION

The (PLL) formulation presented in Chreim *et al.* (2018a) is briefly reviewed here; each blade and its wake is discretized by N helical horseshoe vortices (HHSVs) placed alongside (Figure 1) in a Vortex-Step fashion, with the bound vortices (BVs) placed along the quarter chord line and the control points (CPs) initially placed along the three-quarter chord line; moreover, while part of the HHSVs remains over the blade planform, the other part is shed downstream following an assumed constant pitch helical path, as part of the moderately loaded propeller assumption.

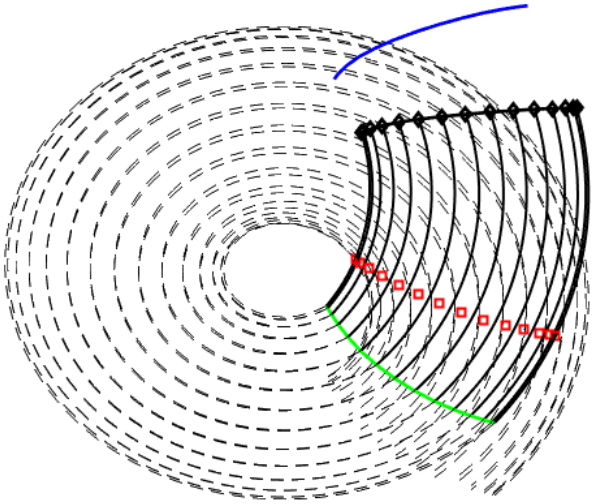

Figure 1. Blade modelled by a series of HHSVs. The solid circumferential lines are part that remains over the planform, while the dashed is the part shed into the freestream.

By lack of analytic expression for the velocities induced by this configuration, each helix can is modelled by N_S segments (Fig. 1) of length δ_w, so as $N_S \to \infty$, $\delta_w \to 0$ and the approximated velocities asymptotically reproduce the exact value. Hence, the velocity $\vec{V}^{b_i b_j}_{VS,ij,k_j k_{j+1}}$ induced by the blade b_j j^{th} segment of vertices k_j and k_{j+1} and circulation $\Gamma^{b_j}_j$ on the blade b_i i^{th} control point can be calculated by equation 1 (Chreim *et al.*, 2018b):

$$\vec{V}^{b_i b_j}_{VS,ij,k_j k_{j+1}} = \frac{\Gamma^{b_j}_j}{4\pi} \frac{\left(r^{b_i b_j}_{ij,k_j} + r^{b_i b_j}_{ij,k_j+1}\right)\left(\vec{r}^{b_i b_j}_{ij,k_j} \times \vec{r}^{b_i b_j}_{ij,k_j+1}\right)}{r^{b_i b_j}_{ij,k_j} r^{b_i b_j}_{ij,k_j+1}\left(r^{b_i b_j}_{ij,k_j} r^{b_i b_j}_{ij,k_j+1} + \vec{r}^{b_i b_j}_{ij,k_j} \cdot \vec{r}^{b_i b_j}_{ij,k_j+1}\right)} \tag{1}$$

The velocity of an entire HHVS $\vec{V}^{b_i b_j}_{HS,ij}$ over i is given by the superposition of the N_S induced velocities:

$$\vec{V}^{b_i b_j}_{HS,ij} = \sum_{k_j=1}^{N_S} \vec{V}^{b_i b_j}_{VS,ij,k_j k_{j+1}} = \frac{\Gamma^{b_j}_j}{4\pi} \vec{v}^{b_i b_j}_{ij} \tag{2}$$

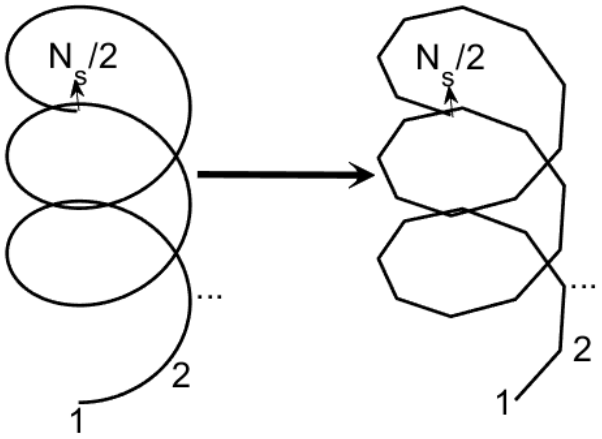

Figure 2. Helix approximated by a series of straight segments.

$$\vec{v}_{ij}^{\,b_i b_j} = \sum_{k_j=1}^{N_S} \frac{\left(r_{ij,k_j}^{b_i b_j} + r_{ij,k_j+1}^{b_i b_j}\right)\left(\vec{r}_{ij,k_j}^{\,b_i b_j} \times \vec{r}_{ij,k_j+1}^{\,b_i b_j}\right)}{r_{ij,k_j}^{b_i b_j} r_{ij,k_j+1}^{b_i b_j}\left(r_{ij,k_j}^{b_i b_j} r_{ij,k_j+1}^{b_i b_j} + \vec{r}_{ij,k_j}^{\,b_i b_j} \cdot \vec{r}_{ij,k_j+1}^{\,b_i b_j}\right)} \tag{3}$$

For a Z bladed propeller rotating at angular speed $\vec{\omega}$, the total velocity $\vec{V}_{P_i^{b_i}}$ at i is the sum of the velocities induced by the $N \times Z$ HHSVs, the free-stream velocity $\vec{V}_\infty$, and the rotating velocity $\vec{V}_{t_i^{b_i}}$:

$$\vec{V}_{P,i}^{b_i} = \vec{V}_\infty + \vec{V}_{t,i}^{b_i} + \sum_{b_j=1}^{N_B}\sum_{j=1}^{N} \vec{V}_{HS,ij}^{b_i b_j} \tag{4}$$

The Pistolesi Boundary Condition (PBC) (Pistolesi, 1937) is necessary to guarantee the zero normal flow requirement; this condition, applied to equation 4 for each CP creates a system of $N \times Z$ whose solution provides the circulation distribution throughout the blades:

$$\mathbf{M_P \Gamma}_P = -\mathbf{W}_{\infty P} \tag{5}$$

in which $\mathbf{M_P}$ is the propeller influence matrix, formed by the blades one-to-one influence submatrices; after $\mathbf{\Gamma_P}$ is obtained, a potential form of the normal section force coefficient can be calculated with the aid of the Kutta-Joukowski Theorem (Chreim *et al.*, 2018a):

$$C_{nPot,i}^{b_i} = \frac{2\Gamma_i^{b_i}\delta l_i^{b_i}\sin\theta_i^{b_i}}{V_{TV_i^{b_i}}\delta A_i^{b_i}} \tag{6}$$

Real $C_n \times \alpha$ foil curves generally do not have slopes of 2π, so the viscous force coefficients $C_{nVis,i}^{b_i}$ are not in agreement with their potential counterparts; an iterative procedure is necessary to adjust the chordwise location of the CPs along the chord lengths c_i, as in equation 8, and make both $C_{n\alpha,i} = \frac{\partial C_{n,i}}{\partial \alpha_i}$ match (Figure 3), an scheme that effectively changes the coefficients of $\mathbf{M_P}$ as the CPs iteratively satisfy the PBC in their new locations:

$$C_{n\alpha,i} = (1-\Omega_i)\, C_{n\alpha,i} + \Omega_i C_{n\alpha Vis,i} \tag{7}$$

$$x_{cp,i} = \left[\frac{1}{2}\frac{C_{n\alpha,i}}{2\pi} + \frac{1}{4}\right] c_i \tag{8}$$

with $0 < \Omega_i \leq 1$. Both $C_{nVis,i}^{b_i}$ and $C_{n\alpha Vis,i}$ are obtained from either numerical or experimental database, and they are generally function of Re and α. Sequentially, the effective angles of attack $\alpha_{eff,i}^{b_i}$, used to update $C_{nVis,i}^{b_i}$, are calculated:

$$\alpha_{eff,i}^{b_i} = \frac{C_{nPot,i}^{b_i}}{C_{n\alpha,i}} - \alpha_{L0,i} \tag{9}$$

And the process described is repeated until both coefficients are equal to within a desired numerical tolerance; after convergence, $C_{n,i}^{b_i}$ and the viscous axial force coefficients $C_{c,i}^{b_i}$, available from the same source of data, are used to calculate the propeller thrust K_T and torque K_Q coefficients:

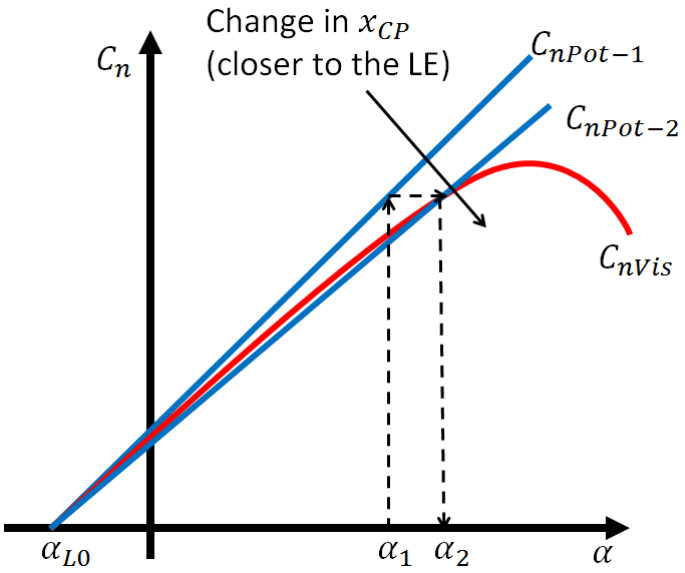

Figure 3. Schematics of the iterative, nonlinear scheme: A change in the chordwise location of the control points alters the slope of the curve $C_n \times \alpha$ accordingly

$$K_T = \frac{\sum_{b_i=1}^{Z}\sum_{i=1}^{N}\left(V_{TV,i}^{b_i}\right)^2 \delta A_i \left[C_{n,i}^{b_i}\cos\left(\beta_{Ind,i}^{b_i}\right) - C_{c,i}^{b_i}\sin\left(\beta_{Ind,i}^{b_i}\right)\right]}{2\rho n^2 D^4} \tag{10}$$

$$K_Q = \frac{\sum_{b_i=1}^{Z}\sum_{i=1}^{N}\left(V_{TV,i}^{b_i}\right)^2 R_i^{b_i}\delta A_i \left[C_{n,i}^{b_i}\sin\left(\beta_{Ind,i}^{b_i}\right) + C_{c,i}^{b_i}\cos\left(\beta_{Ind,i}^{b_i}\right)\right]}{2n^2 D^5} \tag{11}$$

The CPs hydrodynamic pitch angles $\beta_{Ind,i}^{b_i}$ are calculated according to equation 12 (Chreim *et al.*, 2018a), which comes essentially from the basic condition that the geometric pitch $\theta_i^{b_i}$ is the difference between $\alpha_{eff,i}^{b_i}$ and $\beta_{Ind,i}^{b_i}$:

$$\beta_{Ind,i}^{b_i} = \alpha_{eff,i}^{b_i} - \theta_i^{b_i} \tag{12}$$

The wake is shed into the freestream at an angle $\beta_{W,i,k_*}^{b_i}\left(* = \frac{N_s}{2}, \frac{N_{s+1}}{2}\right)$ according to the model proposed by Epps (2017) (Equation 13), whose relation between $\beta_{W,i,k_*}^{b_i}$ and $\beta_{Ind,i}^{b_i}$ and the two projected radii - of the BV edges and the CP -, $R_{i,k_*}^{b_i}$ and $R_i^{b_i}$ respectively, is given by:

$$R_{i,k_*}^{b_i} tan\left(\beta_{w,i,k_*}^{b_i}\right) = R_i^{b_i} tan\left(\beta_{Ind,i}^{b_i}\right) \tag{13}$$

As stated, since equation 13 establishes a constant hydrodynamic pitch typical from optimal circulation distributions, the wake model intrinsically carries the moderately loaded propeller assumption. Additionally, as the hub considerably alters the blade circulation distribution, specially at the inner regions of the blades (Kerwin and Hadler, 2010; Epps, 2017), it has been considered in the formulation through the model proposed by Kerwin, as the author claims that its performs as remarkably as more complex ones (Kerwin and Hadler, 2010).

4. RESULTS

4.1 NACA 66 (TMB Modified Nose and Tail) thickness a = 0.8 camberline 2-D Data comparison

In lifting-line methods, a common practice is the adoption of 2-D C_n and C_c data for blade section distributions; undoubtedly, the more representative is the information about the curve slopes and the zero-lift angles of attack, the more accurate should be the section force and moment distributions that comprise the overall thrust and torque coefficients. Aiming to assess the differences among analytic, numerical, and theoretical results, the NACA 66 (TMB Modified Nose and Tail) thickness with NACA and a = 0.8 camberline has been chosen as benchmark for 2-D data, because it has been

widely used in many propeller geometries (Denny, 1968; Ghose, 2004) and also well characterized (Brockett, 1966). For a given foil maximum thickness-to-chord ratio $\frac{t_0}{c}$ and maximum camber-to-chord ratio $\frac{f_0}{c}$, a known empirical/analytic $C_n \times \alpha$ expression for $Re \geq 6 \times 10^6$ is given as (Brockett, 1966):

$$C_n = 2\pi \left(1 - 0.83\frac{t_0}{c}\right)\left(\alpha + 2.05\frac{f_0}{c}\right) \tag{14}$$

while the C_c is typically assumed to be 0.0085 for such foil family, in spite of the angle of attack, thickness, or camber (Denny, 1968; Epps *et al.*, 2009). The known results from the thin foil theory (Katz and Plotkin, 2001) state that $C_c = 0$ regardless of the geometry and, for a parabolic arc foil, $\frac{\partial C_n}{\partial \alpha} = 2\pi$ and $\alpha_{L0} = -2\frac{f_0}{c}$ such that:

$$C_n = 2\pi \left(\alpha + 2\frac{f_0}{c}\right) \tag{15}$$

For the numerical results, simulations have been carried using the Star-CCM+ commercial software. While the geometries were constructed based on tabulated values for standard thickness and meanline distributions (Carlton, 2012), the domain had approximately 200,000 elements in a trimmed mesh configuration (Fig. 4), with five chord lengths fore and 20 chord lengths aft the foil section, and a total height of 9 chord lengths; the wake refinement used had a spreading angle of approximately 13° and five and a half chord lengths, with the cells in growing in a slow fashion. A steady $K - \omega$ SST model with low Reynolds damping was used, because the range of blade section Reynolds for e model-scale propellers simulated on the PLL were in between 1×10^4 and 1×10^5 orders of magnitude, and the closest-to-the-geometry element was kept sufficiently small for the values of wall y+ be no higher than 1 aside near de leading edge. The convergence criteria were asymptotic for C_n and C_c within a range of 1000 iterations, with maximum differences no higher than 1×10^{-4} and 1×10^{-5}, respectively. The Sdr criterium was also set to reach a minimum value of 1×10^{-5}. For some simulations, the established criteria could not be satisfied due to the foil geometry that, in interaction with the fluid flow, created flow instabilities that depended on the angle of attack, thickness, and camber distributions; in these cases, an averaged value for the nonconverged quantity was set as the output.

Figures 5 and 6 present the comparisons among the three sources of 2-D data for two NACA 66 sections. For the thinnest foil, the section lift curves evidence a satisfying agreement between numerical and experimental data for most of the α range, and only near $\alpha = 5^\circ$ the experimental curve seems to be reaching stall onset, where differences are the highest. Additionally, the difference from these two to the theoretical curve are relatively subtle, increasing with the increase in the absolute value of α; such trends corroborate the appropriateness of the thin-foil theory expression for this case, and any of the three sources used would not produce significant differences.

For the thickest foil, however, the differences among the three curves are significant; as expected, the theoretical curve presents the highest of all slopes, and the analytic expression is the second. Also, the zero-lift angle of attack changes significantly from numerical to analytic, while between analytic and theoretical they are nearly the same. In this case, evidently, the choice of 2-D strongly influences the outcomes for the lifting-line. Additionally, in terms of C_c, none of the three curves agree with one another, but the differences between the simulated values and the other two are more prominent for the thickest foil.

Figure 7 presents a visual comparison between the magnitude of the velocity fields - normalized by the freestream - over both foils. Note that for the thinnest foil, there is a relatively low region of flow detachment near the trailing edge, a thin wake region, and the flow seems well behaved, reasons it is reasonably characterized by both theory and experimental expressions. For the thickest one, on the other hand, the separation region as well as its wake are larger, meaning that flow instabilities are likely to happen sooner and explaining why it seems not be adequately modelled by any of the two means.

4.2 MOD5 propeller $K_T \times J$ and $K_Q \times J$ comparison

In order to compare the influence of the several $C_n \times \alpha$ and $C_c \times \alpha$ curves on the thrust and torque simulated by the proposed PLL, the propeller called MOD5, whose particulars have been currently studied (Esteves *et al.*, 2018; Silva Jr *et al.*, 2019a,b; Chreim *et al.*, 2019), is simulated and compared to experimental data and to numerical data from 3-D CFD simulation performed on Star-CCM+ commercial software. MOD5 is a seven-bladed propeller with quadratic skew distribution that has been conceived to be used in submarines, so it is thought to operate in between moderately and lightly loaded conditions near operation design. The blade outline is presented on Tab. 1, while the propeller schematics is presented on Fig. 8.

The experimental results were obtained from the Cavitation Tunnel of the Institute for Technological Research (IPT) in a relatively large range of advance ratios J (from 0.2 to 1.2, approximately) (Silva Jr *et al.*, 2019b), and the necessary corrections due to the measurement uncertainty and blockage effects of the tunnel were considered following the procedure described by Katsuno and Dantas (Katsuno and Dantas, 2017). The numerical simulations, on the other hand also used the $K - \omega$ SST model and a discretization whose y+ was kept near unit, whereas periodic interfaces were used to minimize computational costs (Esteves *et al.*, 2018). Finally, for all the PLL simulations, $N = 40$, while the Vortex Loop Density

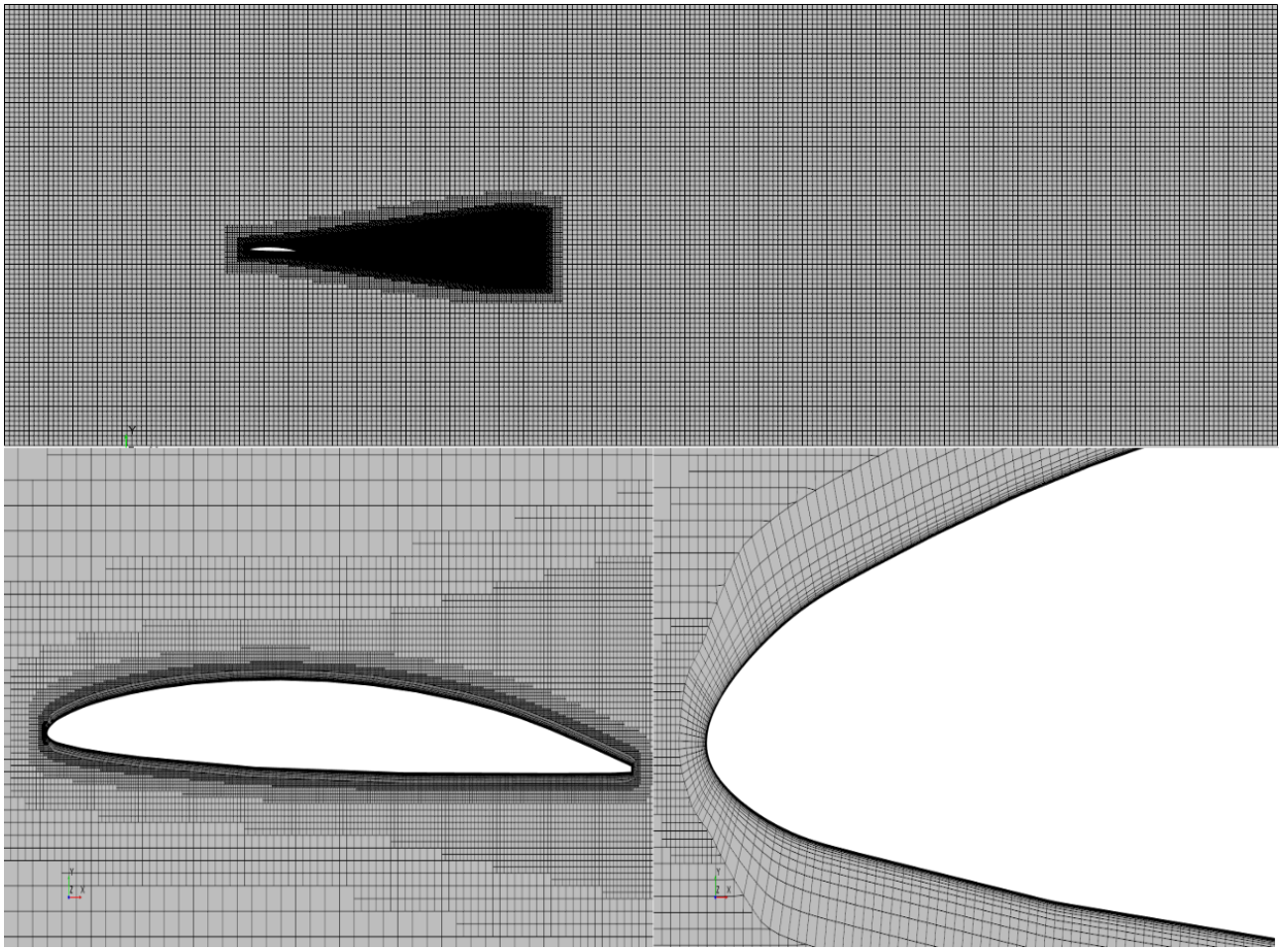

Figure 4. Star-CCM+ CFD domain for the NACA 66 (TMB Modified Nose and Tail) thickness with NACA and a = 0.8 camberline sections simulations

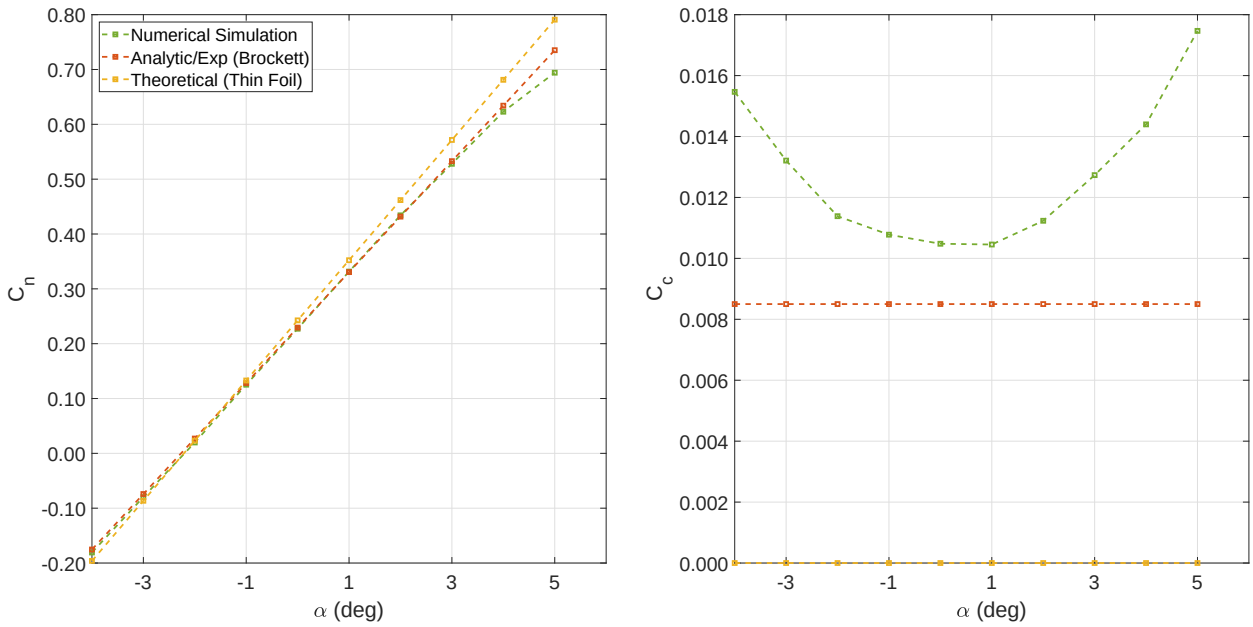

Figure 5. Comparison for $C_n \times \alpha$ (left) and $C_c \times \alpha$ (right) among numerical, analytic/experimental, and theoretical values for a NACA 66 TMB Modified a = 0.8 - $\frac{t_0}{c} = 0.0933$, $\frac{f_0}{c} = 0.0193$.

$VLD = 120$, and the number of helical loops $N_H = 6$ since those values, distributed in a cosine fashion, are enough to

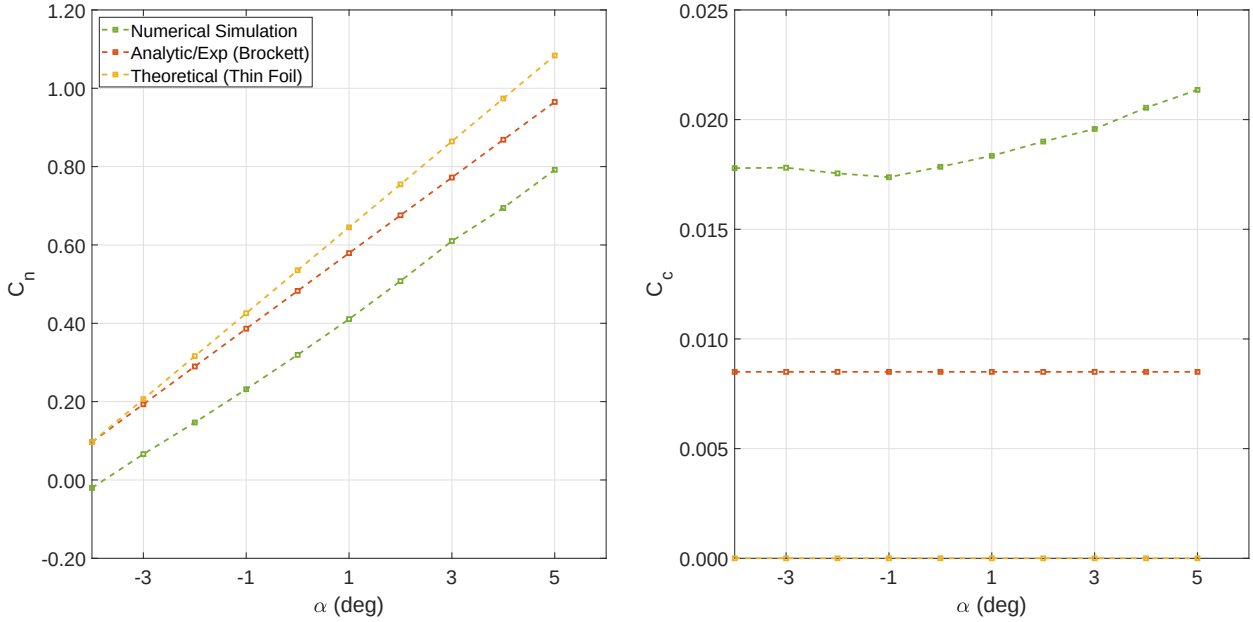

Figure 6. Comparison for $C_n \times \alpha$ (left) and $C_c \times \alpha$ (right) among numerical, analytic/experimental, and theoretical values for a NACA 66 TMB Modified a = 0.8 - $\frac{t_0}{c} = 0.1449$, $\frac{f_0}{c} = 0.0426$.

Table 1. MOD5 Propeller details

Number of blades, Z: 7					
Hub diameter ratio: 0.2					
Expanded Area Ratio: 0.604					
Section mean line: NACA a = 0.8					
Section thickness distrib: NACA66 TMB mod					
Design advance coefficient, J = 0.919					
$\frac{r}{R}$	$\frac{c}{D}$	$\frac{P}{D}$	$\frac{t_0}{c}$	$\frac{f_0}{c}$	θ_S
0.20	0.1812	0.9000	0.1718	0.0000	0.00
0.25	0.1814	1.0530	0.1599	0.0501	-2.73
0.30	0.1830	1.0920	0.1449	0.0426	-4.94
0.40	0.1856	1.1470	0.1213	0.0305	-7.75
0.50	0.1901	1.1970	0.1036	0.0235	-8.44
0.60	0.1945	1.2140	0.0933	0.0193	-7.00
0.70	0.1936	1.2160	0.0919	0.0174	-3.44
0.80	0.1741	1.2040	0.0905	0.0187	2.25
0.90	0.1226	1.1450	0.0891	0.0242	10.06
0.95	0.0821	1.0980	0.0884	0.0335	14.77
1.00	0.0000	1.0440	0.0884	0.0000	20.00

guarantee discretization errors in the order of a few percent (Chreim *et al.*, 2018a). Additionally, the three aforementioned source of 2-D data were used and, for the CFD case, first and second order polynomials were used to extrapolate the values of C_n and C_c for a given angle of attack off the rang of simulations, but the $\frac{t_0}{c}$ and $\frac{f_0}{c}$ have always been interpolated.

From Fig. 9, for the $K_T \times J$ curve, it can be observed the good agreement that both the PLL using either Brockett analytic expression or the CFD 2-D data have with the experimental results, whereas the PLL fed with section data from the thin foil theory presents significant differences; such trends evidence the importance of adequately choosing the source of 2-D data. Moreover, the PLL has differences on average that are in the same order of the full CFD simulations, and they present better agreement specially near the optimum open-water operation advance coefficient $J = 0.9194$, which is an expected trend given the moderately loaded assumption. In terms of $K_Q \times J$, the numerical curves practically overlap, with no significant differences from one another but at lower values of J. They all have some disparity from the experimental values, meaning that none of the formulations adequately modelled the effects of viscosity. Also, between the PLL (2-D thin foil) and the other two, the source of resistive torque is different: with a higher value for thrust for the thin foil data, the higher is the contribution of the induced torque, whereas on the other two cases, part of the torque is

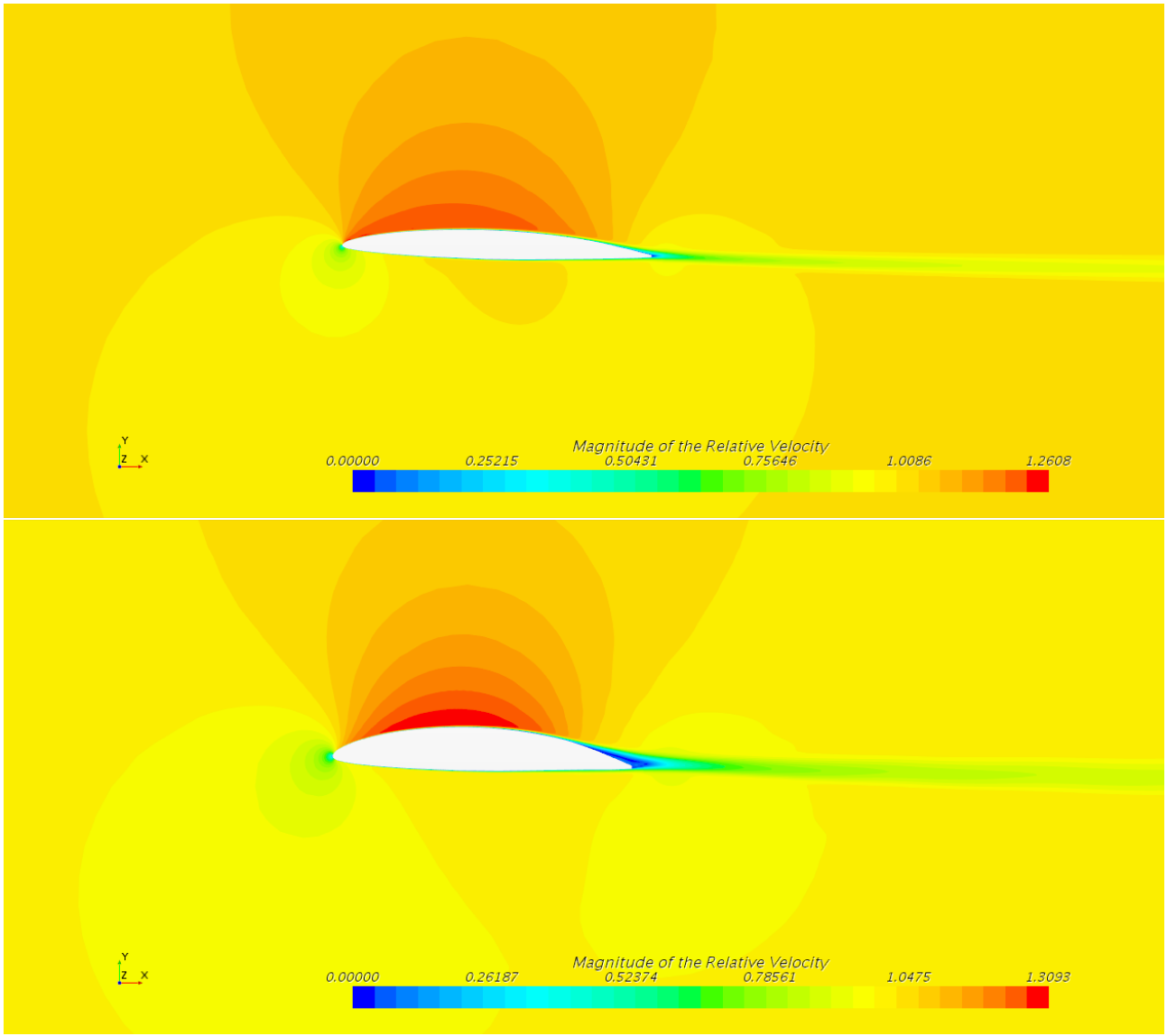

Figure 7. Magnitudes of the velocity fields normalized by the freestream velocity for the NACA 66 TMB Modified a = 0.8 - $\frac{t_0}{c} = 0.0933$, $\frac{f_0}{c} = 0.0193$ (upper) and $\frac{t_0}{c} = 0.1449$, $\frac{f_0}{c} = 0.0426$ (lower).

also originated from the viscous contributions.

5. CONCLUSION

The present paper shows the comparison of three different source of 2-D data (in terms of $C_n \times \alpha$ and $C_c \times \alpha$) that can be used on the proposed propeller lifting-line formulation; the formulation itself has the capability of adequately simulating propellers with rake and skew near optimum operation condition and also of incorporating viscosity on the calculation of thrust and drag, but it is sensitive to the choice of the 2-D data. Sequentially, the three sources are used to obtain the $K_T \times J$ and $K_Q \times J$ curves for the MOD5 propeller, and they are compared to one another and to full CFD simulations and experiments, both carried at the Institute for Technological Research. The outputs show the importance of the 2-D data on the final results of the lifting line - as both the experimental/analytic and numerical sources bring better curves agreement in comparison the theoretical source - and also its accuracy in comparison to full CFD simulations. Hence, for the purpose of preliminary hydrodynamic analysis and hull-propeller design, the proposed formulation, with an adequate choice of 2-D data, seems to provide the same level of accuracy of more sophisticated numerical methods.

6. ACKNOWLEDGEMENTS

This study was financed in part by the Coordenacao de Aperfeicoamento de Pessoal de Nivel Superior - Brasil (CAPES) - Finance Code 001. The authors would like to express their gratitude to both CAPES, under project 1655506,

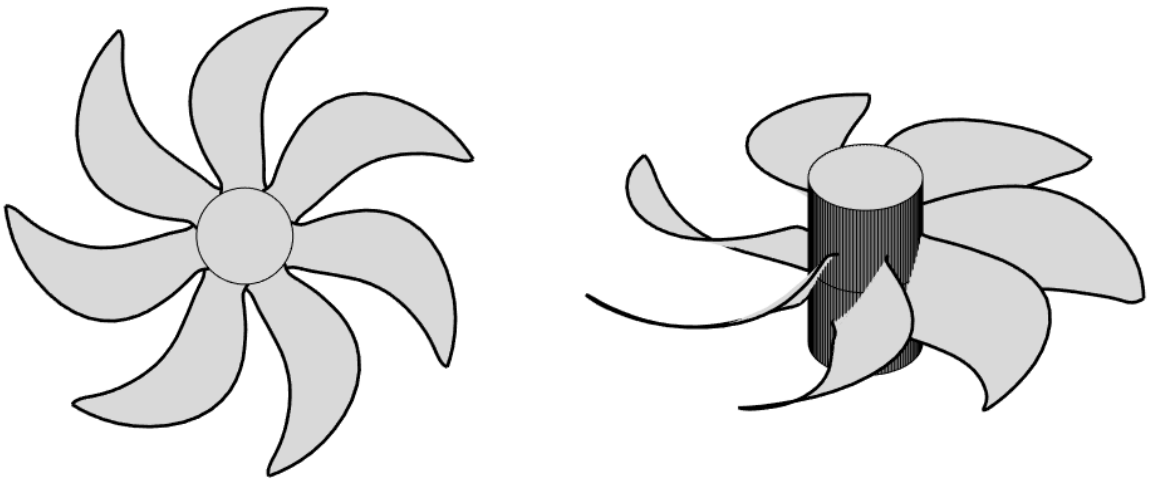

Figure 8. MOD5 Propeller: Propeller schematics

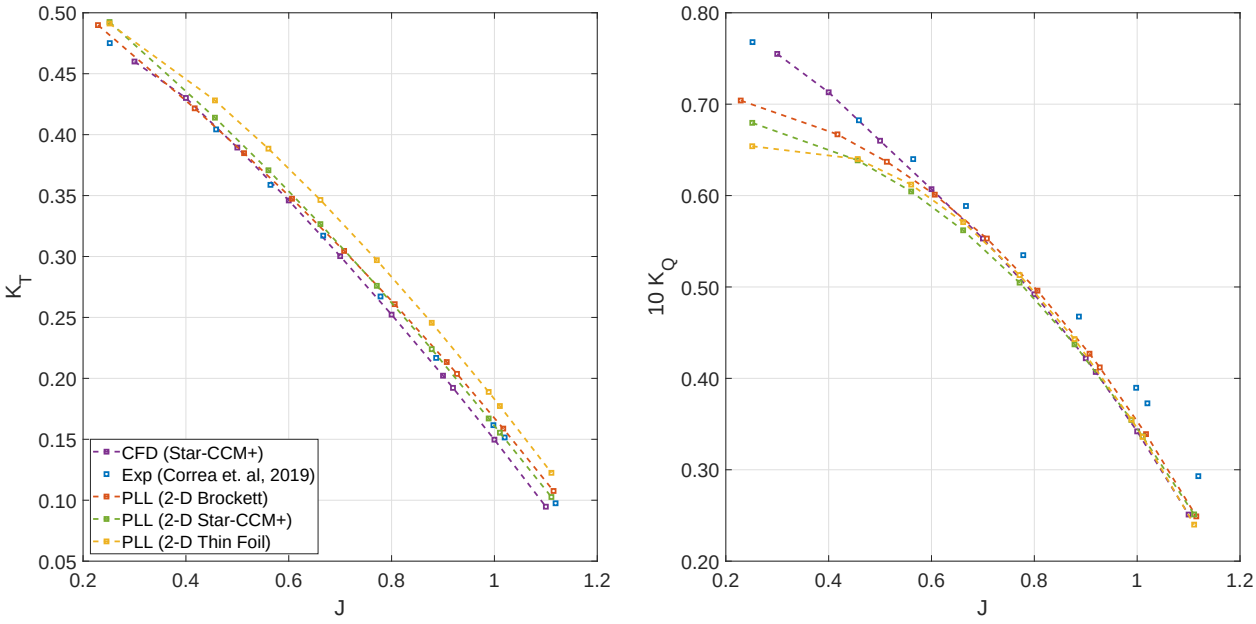

Figure 9. Comparison for $K_T \times J$ (left) and $10K_Q \times J$ (right) among commercial CFD software, experimental data, and the proposed PLL formulation with three different source of 2-D data.

and the Fundacao de Apoio ao Instituto de Pesquisas Tecnologicas (FIPT).

7. REFERENCES

Brockett, T., 1966. "Minimum pressure envelopes for modified naca-66 sections with naca a = 0.8 camber and buships type 1 and type 2 sections". *David Taylor Model Basin Washington DC Hydromechanics Lab*.

Carlton, J., 2012. *Marine propellers and propulsion*. Butterworth-Heinemann.

Chreim, J.R., Esteves, F.R., Pimenta, M.M., Assi, G.R., Dantas, J.L.D. and Kogishi, A.M., 2019. "Validation of a novel

lifting-line method for propeller design and analysis". In *Proceedings of the 14th Practical Design of Ships and Other Floating Structures - PRADS 2019 (Expected)*. Yokohama, Japan.

Chreim, J.R., Dantas, J.L.D., Burr, K.P. and Pimenta, M.d.M., 2017. "Viscous effects assessment through nonlinear lifting-line theory". In *24th ABCM International Congress of Mechanical Engineering*. ABCM - Associacao Brasileira de Engenharia e Ciencias Mecanicas.

Chreim, J.R., de Mattos Pimenta, M., Dantas, J.L.D., Assi, G.R. and Katsuno, E.T., 2018a. "Development of a lifting-line-based method for preliminary propeller design". In *ASME 2018 37th International Conference on Ocean, Offshore and Arctic Engineering*. American Society of Mechanical Engineers, pp. V002T08A008–V002T08A008.

Chreim, J.R., Pimenta, M., Dantas, J.L.D. and Assi, G., 2018b. "Changes in modern lifting-line methods for swept wings and viscous effects". In *2018 Applied Aerodynamics Conference*. p. 3170.

de Souza, S.L., 2005. *Elaboração de uma Metodologia para predição do Coeficiente de Sustentação Máximo de Asas Flapeadas*. Master's thesis, Instituto de Tecnológico de Aeronáutica.

Denny, S.B., 1968. "Cavitation and open-water performance tests of a series of propellers designed by lifting-surface methods". Technical report, DAVID W TAYLOR NAVAL SHIP RESEARCH AND DEVELOPMENT CENTER BETHESDA MD DEPT ....

Epps, B., 2017. "On the rotor lifting line wake model". *Journal of Ship Production and Design*, Vol. 33, No. 1, pp. 31–45.

Epps, B., Chalfant, J., Kimball, R., Techet, A., Flood, K. and Chryssostomidis, C., 2009. "Openprop: An open-source parametric design and analysis tool for propellers". In *Proceedings of the 2009 grand challenges in modeling & simulation conference*. Society for Modeling & Simulation International, pp. 104–111.

Esteves, F.R., Gomes, G.G., Katsuno, E.T. and Dantas, J.L.D., 2018. "Simulation of darpa suboff model propeller hull interaction". In *Proceedings of the 27th International Congress on Waterborne Transportation, Shipbuilding and Offshore Constructions*.

Ghose, J., 2004. *Basic ship propulsion*. Allied publishers.

Katsuno, E. and Dantas, J., 2017. "Analysis of the blockage effect on a cavitation tunnel using cfd tools". In *ASME 2017 38th International Conference on Ocean, Offshore and Arctic Engineering, American Society of Mechanical Engineers*.

Katz, J. and Plotkin, A., 2001. *Low-speed aerodynamics*, Vol. 13. Cambridge University Press.

Kerwin, J.E. and Hadler, J.B., 2010. "Principles of naval architecture series: Propulsion". *The Society of Naval Architects and Marine Engineers (SNAME)*.

Lerbs, H.W., 1952. "Moderately loaded propellers with a finite number of blades and arbitrary distribution of circulation." *Trans SNAME*.

Morgan, W.B., Silovic, V. and Denny, S.B., 1968. "Propeller lifting-surface corrections". Technical report, HYDRO-AND AERODYNAMICS LAB LYNGBY (DENMARK) HYDRODYNAMICS SECTION.

Pepper, R.S. and van Dam, C., 1996. "Design methodology for multi-element high-lift systems on subsonic civil transport aircraft". Technical Report 19960054343, National Aeronautics and Space Administration.

Phillips, W. and Snyder, D., 2000. "Modern adaptation of prandtl's classic lifting-line theory". *Journal of Aircraft*, Vol. 37, No. 4, pp. 662–670.

Pistolesi, E., 1937. "Considerations respecting the mutual influence of systems of airfoils". In *Collected Lectures of the 1937 Principal Meeting of the Lilienthal Society*.

Silva Jr, H.C., Esteves, F.R., Dantas, J.L.D., Moura, A.J.S., Neto, W.N.B., Kogishi, A.M. and Sbragio, R., 2019a. "Experimental and numerical analysis of tip vortex of a darpa suboff auv propeller". In *Proceedings of the 14th Practical Design of Ships and Other Floating Structures - PRADS 2019 (Expected)*. Yokohama, Japan.

Silva Jr, H.C., Esteves, F.R., Dantas, J.L.D., Moura, A.J.S., Neto, W.N.B., Kogishi, R.C.S.A.M. and Sbragio, R., 2019b. "Tip vortex comparison of a darpa suboff auv propeller: Experimental and numerical methods". In *Proceedings of the 14th Practical Design of Ships and Other Floating Structures - PRADS 2019 (Expected)*. Yokohama, Japan.

Weissinger, J., 1947. "The lift distribution of swept-back wings". Technical report, NATIONAL ADVISORY COMMITEE FOR AERONAUTICS.

8. RESPONSIBILITY NOTICE

The authors are the only responsible for the printed material included in this paper.